pathogens

MDPI

Article

Molecular Characteristics and Immunogenicity Evaluation of the 14-3-3 Protein of *Strongyloides stercoralis*

Qing Wen [1,†], Qiuhua Bai [2,†], Yunliang Shi [2,†], Xiaodan Chen [3], Jiayin Lv [4], Jiayue Sun [5], Lili Tang [2], Shanshan He [2], Xiaoyin Fu [2,*] and Dengyu Liu [2,*]

[1] Department of Basic Medical Sciences, Clinical College of Anhui Medical University, Hefei 230031, China; wenqing06012024@163.com
[2] Parasitology Department, School of Basic Medical Sciences, Guangxi Medical University, Nanning 530021, China; bqiuhua@outlook.com (Q.B.); syunliang2008@sr.gxmu.edu.cn (Y.S.); tanglili@163.com (L.T.); 119210588@163.com (S.H.)
[3] Liuzhou People's Hospital Affiliated to Guangxi Medical University, Liuzhou 545006, China; chenxiaodan.research@outlook.com
[4] Women's Hospital School of Medicine Zhejiang University, Hangzhou 310006, China; lvjiayin000@gmail.com
[5] Shenzhen Second People's Hospital Dapeng Hospital, Shenzhen 518000, China; sunjiayuesjy@outlook.com
* Correspondence: fuxyin@outlook.com (X.F.); 330005@sr.gxmu.edu.cn (D.L.)
† These authors contributed equally to this work.

Abstract

Strongyloidiasis is an important parasitic disease, and characterizing the antigenic properties of parasite-derived proteins and the host immune responses they elicit may contribute to a better understanding of host–parasite immune interactions. The highly conserved 14-3-3 proteins have demonstrated immunogenicity in various parasites; however, the immunological characteristics of the *Strongyloides stercoralis* 14-3-3 protein (Ss14-3-3) warrant further investigation. This study aimed to systematically characterize the molecular properties and immunogenicity of Ss14-3-3 and investigate the associated host immune responses. The *Ss14-3-3* gene was cloned, and recombinant Ss14-3-3 (rSs14-3-3) was expressed and purified using a eukaryotic expression system. Its antigenic characteristics and immunogenicity were evaluated through bioinformatic analysis, patient serum recognition, mouse immunization, and splenic transcriptome sequencing. Ss14-3-3 is a hydrophilic protein comprising 245 amino acids, with 12 predicted B-cell epitopes. Sera from infected patients recognized rSs14-3-3. Immunization with rSs14-3-3 formulated with Freund's adjuvant induced significantly increased antigen-specific IgG1 and IgG2a responses in mice, which progressively increased during immunization. Transcriptomic analysis identified 36 differentially expressed genes, and enrichment analysis of these genes highlighted heme- and porphyrin-related processes, while gene set enrichment analysis of the ranked transcriptome identified enrichment of gene sets associated with B-cell activation and lymphocyte differentiation. These findings extend the characterization of rSs14-3-3 immunogenicity by demonstrating human serum recognition and immunization-induced antibody responses.

Keywords: *Strongyloides stercoralis*; 14-3-3 protein; recombinant antigen; immunogenicity; humoral immune response; splenic transcriptomics

Check for updates

Academic Editor: Fabrizio Bruschi

Received: 5 October 2026
Revised: 11 November 2026
Accepted: 11 November 2026
Published: 18 November 2026

Copyright: © 2026 by the authors. Licensee MDPI, Basel, Switzerland. This article is an open access article distributed under the terms and conditions of the Creative Commons Attribution (CC BY) license.

1. Introduction

Strongyloidiasis is a neglected soil-transmitted helminth infection of global public health importance, with an estimated 613.9 million people infected worldwide in 2017 [1]. Current treatment relies primarily on ivermectin, with albendazole used as an alternative.

Nevertheless, missed diagnosis, treatment failure, persistent infection, and recurrence remain important clinical challenges. Moreover, immunocompromised individuals are at risk of developing hyperinfection syndrome or disseminated strongyloidiasis [2,3].

Therefore, in addition to improving diagnosis and conventional pharmacological control, the identification of parasite-derived antigens with potential applications in immunoprophylaxis and diagnostic development remains important. Parasite-derived proteins participate in parasite growth and development, immune evasion, metabolic regulation, and host–parasite interactions, and therefore represent promising targets for vaccine development and diagnostic biomarker discovery [4,5].

The 14-3-3 protein family comprises highly conserved acidic regulatory proteins that generally function as dimers and participate in multiple signaling pathways through interactions with phosphorylated ligands [6]. A number of parasite-derived 14-3-3 proteins can be recognized by the host immune system and have been shown to induce humoral and/or cellular immune responses in different animal models [7]. These findings suggest that parasite 14-3-3 proteins may serve as promising targets for immunological investigation, although the patterns of immune responses elicited by these proteins vary among parasite species and experimental systems.

Masoori et al. [8] showed that recombinant Ss14-3-3 was recognized by antibodies in sera from patients with strongyloidiasis. Recombinant Ss14-3-3 has previously been characterized by Sánchez-Palencia et al. [9]. Bacterially expressed rSs14-3-3 formulated with an adjuvant adaptation system (ADAD) exhibited immunomodulatory effects in mice but did not confer protection against subsequent experimental *Strongyloides venezuelensis* infection. The serological findings in that study were obtained from experimentally infected mice and did not establish diagnostic performance in humans. Further investigation is warranted to characterize human serum recognition and the host responses associated with Ss14-3-3 immunization under additional experimental conditions.

Building on this previous work, the present study expressed rSs14-3-3 in *Pichia pastoris* X33 and evaluated its recognition by human sera, antigen-specific IgG1 and IgG2a responses following immunization in BALB/c mice, and associated whole-spleen transcriptional changes. These complementary analyses extend the characterization of Ss14-3-3 antigenicity and immunogenicity and identify host transcriptional responses for subsequent functional investigation.

2. Materials and Methods

2.1. Parasites and Serum Samples

Collection and use of clinical samples were approved by the Ethics Committee of Guangxi Medical University (approval no. 20210049), and all procedures were conducted in accordance with the principles of the Declaration of Helsinki. All animal experiments, including mouse immunization and euthanasia, were approved by the Animal Ethics Committee of Guangxi Medical University (approval no. 202403005), and all animal care and experimental procedures complied with the institutional guidelines for laboratory animal welfare. The *S. stercoralis* isolate and serum samples used in this study were stored at −80 °C in the Department of Parasitology, Guangxi Medical University, Nanning, China. Serum samples included those from seven patients with strongyloidiasis, three patients with clonorchiasis, four patients with schistosomiasis, and three healthy individuals. Third-stage filariform larvae (L3) of *S. stercoralis* were obtained by culturing fecal specimens collected from confirmed patients. Morphological characteristics of the parasites were examined microscopically, and species identification was further confirmed by amplification of the 18S rDNA HVR-IV region and the mitochondrial *cox1* gene (Figures 1A and S1A,B).

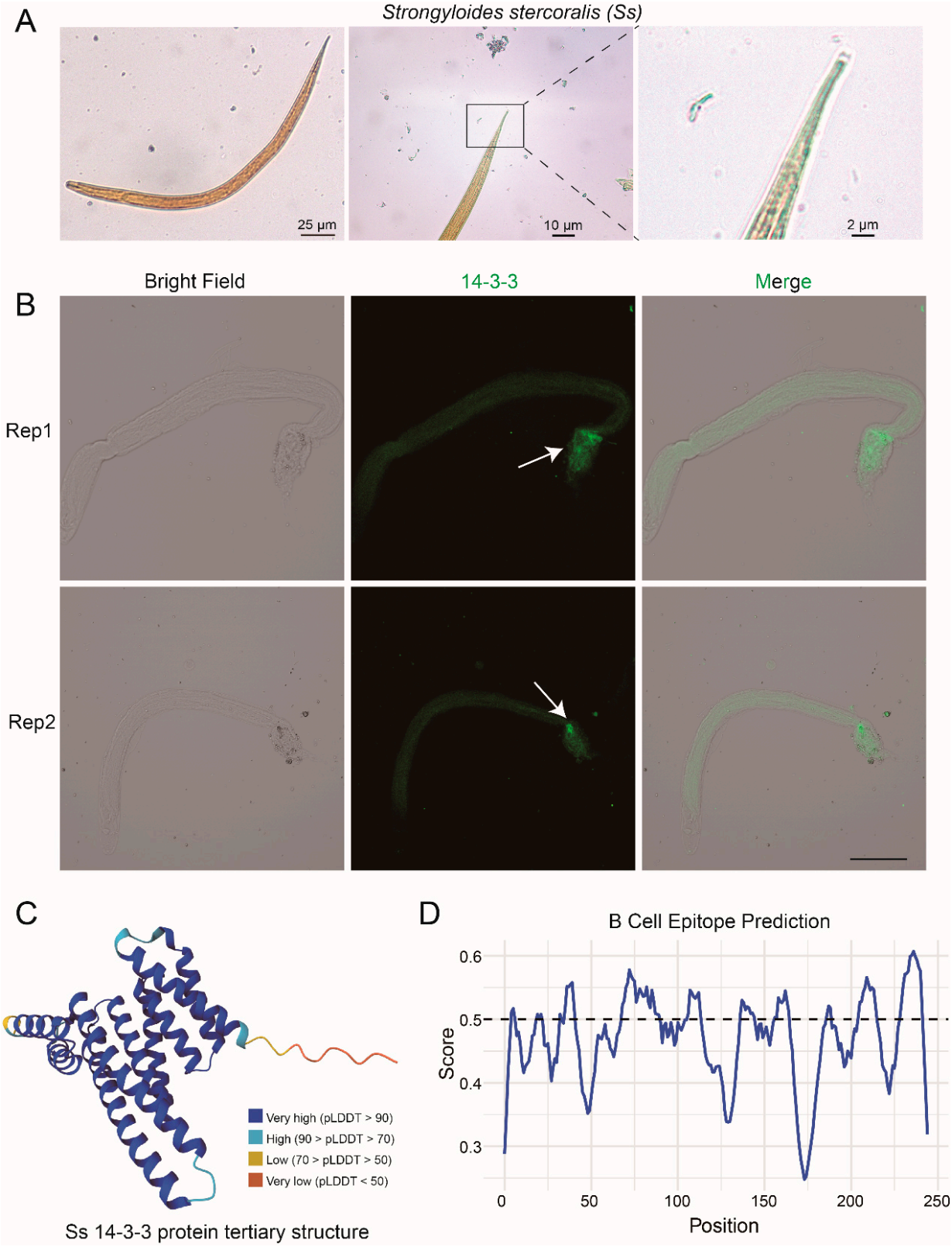


Figure 1. Characterization of the 14-3-3 protein of *Strongyloides stercoralis*. (**A**) The morphological characteristics of *Strongyloides stercoralis*. Scale bars are presented in each image. (**B**) Confocal images of 14-3-3 protein staining in *Strongyloides stercoralis*. White arrows highlight the regions with strong fluorescence signals of the 14-3-3 protein. Two replicate samples (Rep1 and Rep2) are shown. Scale bars, 100 μm. (**C**) *Strongyloides stercoralis* 14-3-3 protein tertiary structure. The predicted local distance difference test (pLDDT) indicates per-residue model confidence. Some regions below 50 pLDDT may be unstructured in isolation. (**D**) Prediction of linear B-cell epitopes for *Strongyloides stercoralis*

14-3-3 protein. The y-axis shows for each residue the correspondent score (averaged in the specified window). The larger score for the residues might be interpreted as that the residue might have a higher probability to be part of epitope (those residues > 0.5).

2.2. Immunofluorescence Staining and Localization

To determine the tissue distribution of Ss14-3-3 within the parasite, worms were collected and fixed with 4% paraformaldehyde. Following washing with PBS, samples were permeabilized with 0.2% Triton X-100. The worms were blocked with 5% bovine serum albumin (BSA) for 1 h at room temperature and subsequently incubated overnight at 4 °C with polyclonal anti-Ss14-3-3 antibodies at a dilution of 1:80. After extensive washing with PBS, samples were incubated with the appropriate fluorescence-conjugated secondary antibody at a dilution of 1:1000 for 1 h at room temperature in the dark. Nuclei were counterstained with DAPI. After washing, the worms were mounted on glass slides using antifade mounting medium and examined using laser-scanning confocal microscopy. Either preimmune serum at the same dilution or omission of the primary antibody were used as negative controls. All samples were imaged using identical microscope settings to allow comparison of Ss14-3-3 fluorescence signals on the parasite surface and within internal tissues.

2.3. Gene Cloning and Vector Construction

Parasite tissues were ground in liquid nitrogen and homogenized in 1 mL of TRIzol reagent. RNA was extracted by chloroform extraction, isopropanol precipitation, and washing with 75% ethanol. The RNA pellet was dissolved in DEPC-treated water. RNA concentration and purity were assessed using a NanoDrop spectrophotometer (Thermo Fisher Scientific, Waltham, MA, USA), with an A260/A280 ratio ≥ 1.8 considered acceptable. RNA integrity was further evaluated by 1% agarose gel electrophoresis, with a 28S/18S rRNA ratio ≥ 2.0 considered acceptable. cDNA synthesis was performed using the PrimeScript RT reagent kit (Takara Bio, Shiga, Japan) according to the manufacturer's instructions.

Primers for amplification of the target Ss14-3-3 gene were synthesized by Sangon Biotech. The forward primer was 5′-GACTGGTTCCAATTGACAAGC-3′, and the reverse primer was 5′-GGCAAATGGCATTCTGACAT-3′. An EcoRI restriction site and a 6 × His tag were introduced at the 5′ end, whereas a NotI restriction site was incorporated at the 3′ end. The PCR product was digested with EcoRI and NotI and ligated into the pPICZαB vector. The recombinant plasmid was transformed into *Escherichia coli* DH5α competent cells. Positive colonies were selected and confirmed by Sanger sequencing.

2.4. Recombinant Protein Expression and Purification

The *Pichia pastoris* X33 strain was purchased from Sangon Biotech (Shanghai) Co., Ltd. (Shanghai, China). The linearized recombinant plasmid was introduced into yeast cells by electroporation, and Mut^+ transformants were selected. Individual colonies were cultured in 10 mL of BMGY medium at 30 °C and 250 rpm for 16 h. Cells were harvested by centrifugation and resuspended in BMMY medium. Recombinant protein expression was induced by supplementation with 0.5% (v/v) methanol every 12 h for a total of 72 h. Following induction, cultures were centrifuged at 12,000× g for 5 min, and the supernatants were collected and stored at −80 °C. Recombinant protein was purified by nickel-affinity chromatography. Culture supernatants were filtered through a 0.22 μm membrane and loaded onto Ni-NTA resin. Bound proteins were sequentially eluted using Tris-HCl buffer (pH 7.4) containing 20, 50, or 500 mM imidazole. Fractions eluted with 500 mM imidazole were collected, dialyzed against Tris-HCl buffer at 4 °C with three buffer changes, concentrated using polyethylene glycol, aliquoted, and stored at −80 °C.

2.5. Mouse Immunization

Six-to-eight-week-old BALB/c mice were randomly assigned into three groups (n = 5 per group): a PBS control group, an adjuvant control group, and an Ss14-3-3 immunization group. Mice were immunized by multiple-site subcutaneous injection. For the primary immunization, 50 μg of Ss14-3-3 protein was emulsified with an equal volume of complete Freund's adjuvant. Booster immunizations were administered at weeks 2 and 4 using incomplete Freund's adjuvant, with the antigen dose reduced by half. Blood samples were collected from the tail vein before immunization at weeks 0, 2, and 4, and before sacrifice at week 6. Serum samples were stored at −80 °C until further analysis.

2.6. Western Blotting

A 200 μL aliquot of protein-containing supernatant was subjected to trichloroacetic acid precipitation and mixed with 20 μL loading buffer boiled to denature the proteins. Proteins were separated by 12% SDS-PAGE at 80 V for 15 min followed by 120 V for 40 min, and subsequently transferred to PVDF membranes at a constant current of 300 mA for 90 min. Mouse anti-His-tag antibody was used as the primary antibody at a dilution of 1:5000, and HRP-conjugated goat anti-mouse IgG was used as the secondary antibody at a dilution of 1:10,000. Signals were visualized using enhanced chemiluminescence, and band intensities were quantified using ImageJ software (version 1.53t).

2.7. ELISA

Recombinant Ss14-3-3 protein (40 ng/μL) was used to coat 96-well plates overnight at 4 °C. The plates were blocked with 5% fetal bovine serum for 1 h at 37 °C. Serum samples were diluted 1:100 and incubated overnight at 4 °C. HRP-conjugated secondary antibodies diluted 1:10,000 were subsequently added and incubated for 1 h at 37 °C. Following incubation with TMB substrate for 10 min, absorbance was measured at 450 nm. The cut-off value for indirect ELISA was defined as the mean OD of negative control sera plus one standard deviation ($\overline{X}_{\text{negative}}$ + 1SD). For exploratory classification of ELISA reactivity, the positivity cutoff was defined as the mean OD450 of the three healthy control sera plus one standard deviation.

2.8. Transcriptome Sequencing and Analysis

Transcriptome sequencing was performed by Novogene. Spleen tissues were collected from five mice per group to provide backup samples in case of unsuccessful sample processing. RNA sequencing was performed on samples from three mice in the rSs14-3-3 immunization group and three mice in the adjuvant control group, with each mouse representing one independent biological replicate (n = 3 per group). Samples from different mice were processed separately without pooling. Mouse spleen tissues were ground to a fine powder in liquid nitrogen, and total RNA was extracted using TRIzol reagent (Thermo Fisher Scientific). RNA libraries were constructed and sequenced on an Illumina NovaSeq platform (Illumina, San Diego, CA, USA) using 150 bp paired-end sequencing. Raw sequencing data were subjected to quality control using FastQC. Reads were aligned using HISAT2, gene-level read counts were obtained using featureCounts, and differential expression analysis was performed using DESeq2. Functional enrichment analyses were performed using the Gene Ontology (GO; https://geneontology.org/) and Kyoto Encyclopedia of Genes and Genomes (https://www.kegg.jp/) databases. Gene set enrichment analysis (GSEA) was performed using the fgsea package (version 1.38.0). Genes were ranked in descending order according to their signed log2 fold change in the rSs14-3-3 immunization group relative to the adjuvant control group. Gene-set p-values were adjusted using the Benjamini–Hochberg method, and gene sets with FDR < 0.05 were considered significantly enriched.

2.9. Statistical Analysis

Statistical analyses were performed according to the experimental design. Differences in antibody reactivity between patients with strongyloidiasis and healthy controls were analyzed using Student's *t*-test. For mouse immunization experiments, differences in antigen-specific IgG1 and IgG2a responses among the experimental groups were analyzed separately at each sampling time point using one-way analysis of variance (ANOVA), followed by Tukey's multiple comparisons test. Differential gene expression analysis was performed using DESeq2. Genes with an unadjusted p-value < 0.05 and $|\log2FC| > 0.5$ were classified as exploratory candidates. For the FDR-controlled analysis, gene-level p-values were adjusted using the Benjamini–Hochberg method, and genes with FDR < 0.05 and $|\log2FC| > 0.5$ were classified as statistically significant differentially expressed genes.

3. Results

3.1. Molecular Characterization and Localization of the Strongyloides stercoralis 14-3-3 Protein

Immunofluorescence staining demonstrated that Ss14-3-3-associated fluorescence signals were distributed both on the surface and within internal tissues of *S. stercoralis*. Relatively strong fluorescence signals were observed in the anterior region of the parasite, whereas weaker signals were detected in the oral cavity, esophagus, and intestine (Figure 1B), indicating differential tissue distribution of Ss14-3-3.

ProtParam analysis indicated that Ss14-3-3 comprises 245 amino acids and has a predicted molecular mass of 27.93 kDa. Other physicochemical properties are summarized in Table S1. Hydropathy analysis showed that the hydrophobicity scores of most regions were below zero, suggesting that Ss14-3-3 is predominantly hydrophilic (Figure S2A). SOPMA analysis predicted that the secondary structure of Ss14-3-3 is dominated by α-helices, involving 166 amino acid residues and accounting for 67.76% of the protein. Random coils, extended strands, and β-turns accounted for 22.45%, 8.16%, and 1.63%, respectively (Figure S2B). The tertiary structure predicted using AlphaFold similarly showed a predominantly α-helical folding pattern (Figure 1C).

TMHMM Server v2.0 predicted no transmembrane domain, and SignalP 6.0 predicted no classical signal peptide in Ss14-3-3 (Figure S2C,D). NetPhos predicted a total of 41 potential phosphorylation sites, including 25 serine, eight threonine, and eight tyrosine residues (Figure S2E).

Phylogenetic analysis showed that Ss14-3-3 clustered relatively closely with the 14-3-3 protein of *Trichinella spiralis*, whereas greater evolutionary distances were observed between Ss14-3-3 and the human and mouse 14-3-3 proteins included in the analysis (Figure S2F). Prediction of linear B-cell epitopes identified 12 candidate epitope regions (Figure 1D and Table S2), providing candidate sequences for subsequent screening and experimental validation.

3.2. Eukaryotic Expression and Purification of Recombinant Ss14-3-3

PCR amplification using *S. stercoralis* cDNA as the template generated a specific band of approximately 750 bp, consistent with the expected size of the *Ss14-3-3* open reading frame (738 bp) (Figure S3A). Sequencing confirmed that the inserted sequence was identical to the Ss14-3-3 sequence deposited in GenBank (Figure S4), verifying successful construction of the recombinant expression plasmid.

After transformation of the recombinant plasmid into *P. pastoris* X33 and induction of protein expression, a target protein of approximately 30 kDa was detected in the culture supernatant. Protein expression increased with induction time and was relatively high after 72 h (Figures 2A and S3B,C). Following Ni-affinity purification and stepwise imidazole elution, the target protein was predominantly detected in fractions eluted with 500 mM

imidazole (Figure 2B). Western blotting revealed a specific band of approximately 30 kDa (Figure 2C). Mass spectrometric analysis demonstrated 96.3% peptide coverage of the reference Ss14-3-3 amino acid sequence (Figure 2D and Table S3), confirming the identity of recombinant Ss14-3-3.

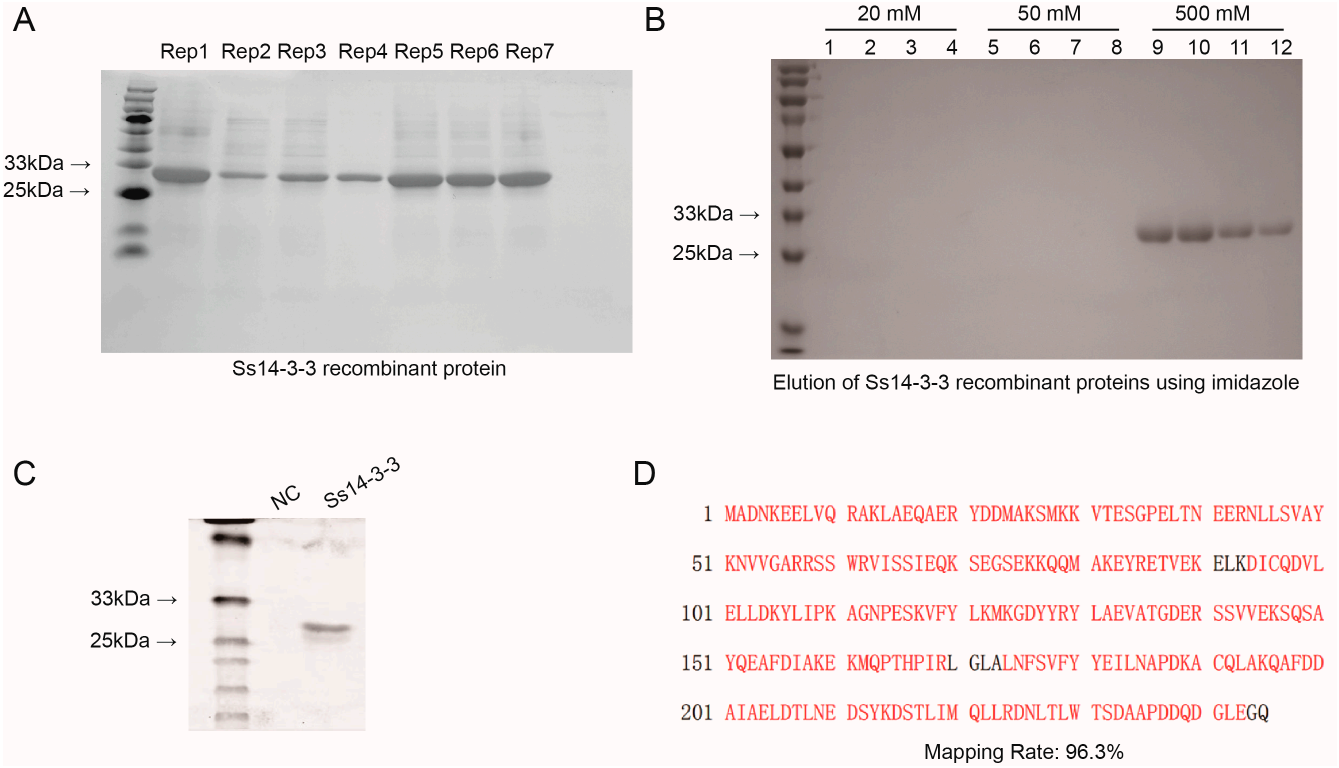


Figure 2. Eukaryotic expression and characterization of recombinant Ss14-3-3 protein. (**A**) Expression of *Strongyloides stercoralis* (Ss) 14-3-3 recombinant protein using SDS-PAGE. The seven lanes represent seven replicate samples (Rep1-7). (**B**) SDS-PAGE analysis of purified *Strongyloides stercoralis* (Ss)14-3-3 recombinant protein. The purified protein was verified using SDS-PAGE after elution with three different concentrations of imidazole (20, 50, 500 mM). (**C**) Western blot analysis of purified *Strongyloides stercoralis* (Ss)14-3-3 recombinant protein. (**D**) Peptide coverage of recombinant Ss14-3-3 protein identified by mass spectrometry. Red regions indicate peptide sequences matched to the target protein.

3.3. Recognition of rSs14-3-3 by Human Sera and Antibody Responses in Immunized Mice

To determine whether antibodies generated during natural infection recognize rSs14-3-3, an indirect ELISA using recombinant Ss14-3-3 as the coating antigen was performed using sera from patients with strongyloidiasis and healthy controls. Serum IgG, IgG1, and IgG2 reactivity against rSs14-3-3 was significantly higher in patients infected with *S. stercoralis* than in healthy controls (Figure 3A–C), indicating the presence of specific antibodies capable of recognizing rSs14-3-3 during natural infection.

To further examine the specificity of serum recognition, IgG reactivity to rSs14-3-3 was assessed using sera from patients with clonorchiasis and schistosomiasis. Positive reactions were observed in all three clonorchiasis samples (3/3, 100%) and two of the four schistosomiasis samples (2/4, 50%). The corresponding group mean OD450 values were 0.403 ± 0.066 and 0.109 ± 0.037, respectively (mean ± SD; Supplementary Table S4). These findings suggest potential cross-reactivity with sera from patients with other helminth infections.

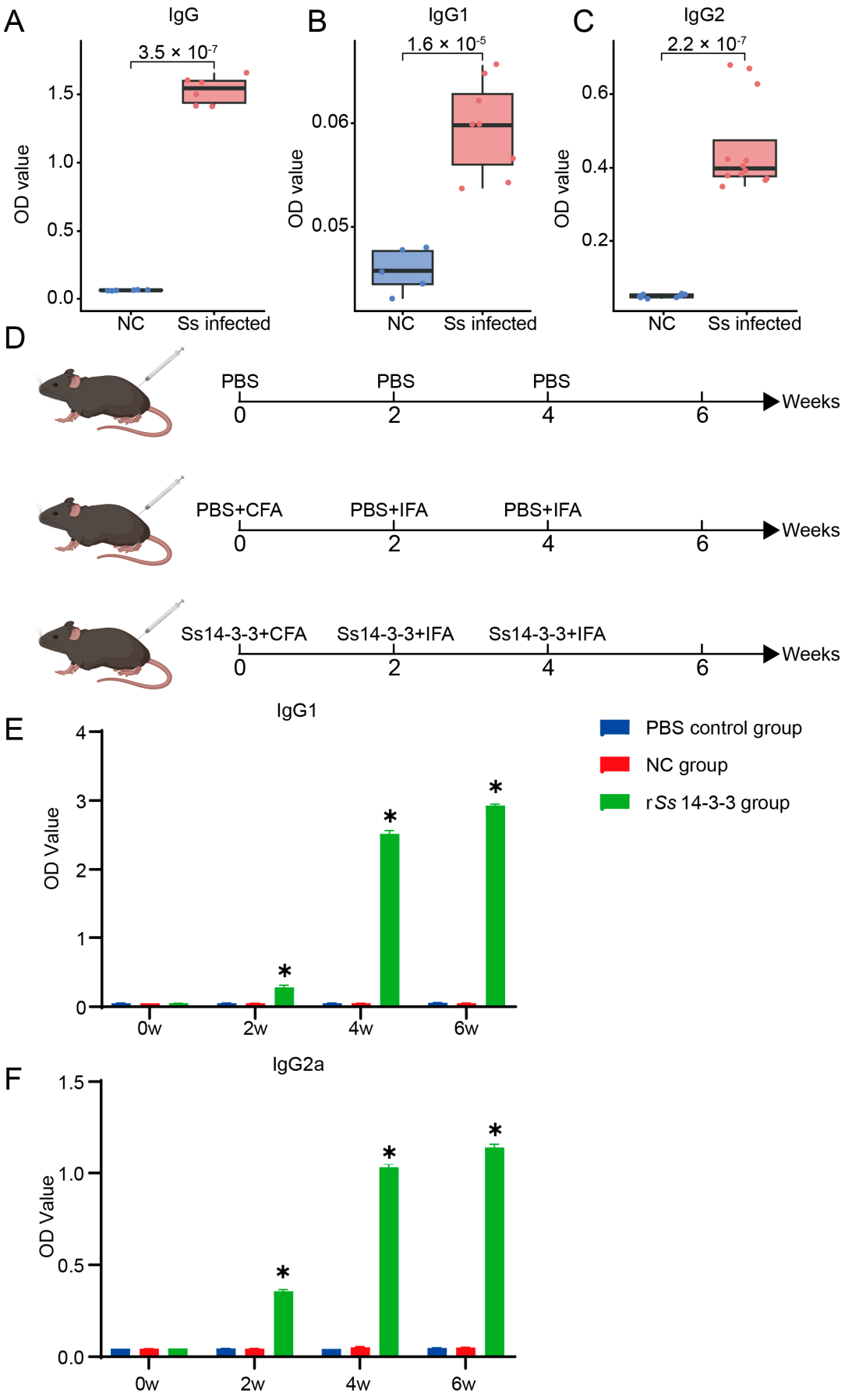


Figure 3. Recognition of rSs14-3-3 by human sera of the *Strongyloides stercoralis* (Ss) 14-3-3 protein. (**A**–**C**) Serum IgG, IgG1, and IgG2 reactivity against recombinant S. stercoralis 14-3-3 protein (rSs14-

3-3) in patients with strongyloidiasis and healthy controls. Each dot represents an individual serum sample. Differences between the two groups were analyzed using Student's *t*-test. (**D**) Schematic illustration of *Strongyloides stercoralis* (Ss) 14-3-3 recombinant protein immunization animal experiment (see Methods). (**E**,**F**) Serum levels of rSs14-3-3-specific IgG1 and IgG2a in mice following immunization. The adjuvant control group received Freund's adjuvant without rSs14-3-3, whereas the rSs14-3-3 group received rSs14-3-3 formulated with Freund's adjuvant. Differences among groups were analyzed using one-way ANOVA, followed by Tukey's multiple-comparisons test. Asterisk (*) indicates a statistically significant difference with $p < 0.0001$.

The ability of rSs14-3-3 to elicit antibody responses was subsequently evaluated in BALB/c mice immunized with the recombinant protein formulated with Freund's adjuvant (Figure 3D). Beginning at week 2 after primary immunization, antigen-specific IgG1 and IgG2a responses were significantly higher in the rSs14-3-3 group than in the PBS and adjuvant control groups. Both antibody subclasses increased progressively at subsequent time points (Figure 3E,F), supporting the immunogenicity of rSs14-3-3 under the tested immunization conditions.

3.4. Transcriptomic Profiling of Spleens from rSs14-3-3-Immunized Mice

To characterize splenic transcriptional alterations associated with rSs14-3-3 immunization, RNA sequencing was performed on whole-spleen tissues from mice receiving rSs14-3-3 formulated with Freund's adjuvant and mice receiving adjuvant alone.

Compared with the adjuvant control group, using an exploratory threshold of $p < 0.05$ and $|\log2FC| > 0.5$, 404 candidate genes were identified, including 169 upregulated and 235 downregulated genes (Figure 4A). After Benjamini–Hochberg correction for multiple testing, 36 genes met the criteria of false discovery rate (FDR) < 0.05 and $|\log2FC| > 0.5$ (Supplementary Table S5). *Bach2* met the adjusted significance threshold in the RNA-seq analysis, whereas *Cxcr4* was identified only in the exploratory analysis (FDR = 0.063). However, RT-qPCR analysis showed changes in the expression of both genes, although the direction of these changes differed from that observed in the RNA-seq analysis (Figure 4B,C).

GO over-representation analysis of the 36 FDR-significant genes identified enriched terms related to hydrogen peroxide metabolism, tetrapyrrole biosynthesis, and porphyrin-containing compound metabolism (Figure S5A and Supplementary Table S6). Several prominent transcriptional differences involved erythroid-associated genes, including *Alas2*, *Hbb-bt*, and *Hbb-bs* (Supplementary Tables S5 and S6).

The differentially expressed genes also included multiple immunoglobulin-related genes in 404 exploratory genes. Functional enrichment analysis of these genes indicated significant enrichment in biological processes related to adaptive immune response, B-cell-mediated immunity, immune effector processes, and immunoglobulin-mediated immune responses (Figure 4D and Supplementary Table S7). GO enrichment analysis of all differentially expressed genes further revealed enrichment in terms associated with B-cell activation, adaptive immune response, and positive regulation of the MAPK cascade (Figure 4E,F).

GSEA further revealed that positive enrichment was observed for B-cell activation, lymphocyte differentiation, and 14-3-3 protein binding (Figure S5B and Supplementary Table S8). Negative enrichment was observed for gene sets associated with chromosome segregation and nuclear division. The GSEA findings supported the corresponding biological themes identified in the exploratory enrichment analysis.

Collectively, these analyses identified immunization-associated transcriptional changes in whole spleen involving immune-related gene sets and erythroid-associated processes. The B-cell-related enrichment represents a tissue-level transcriptional association.

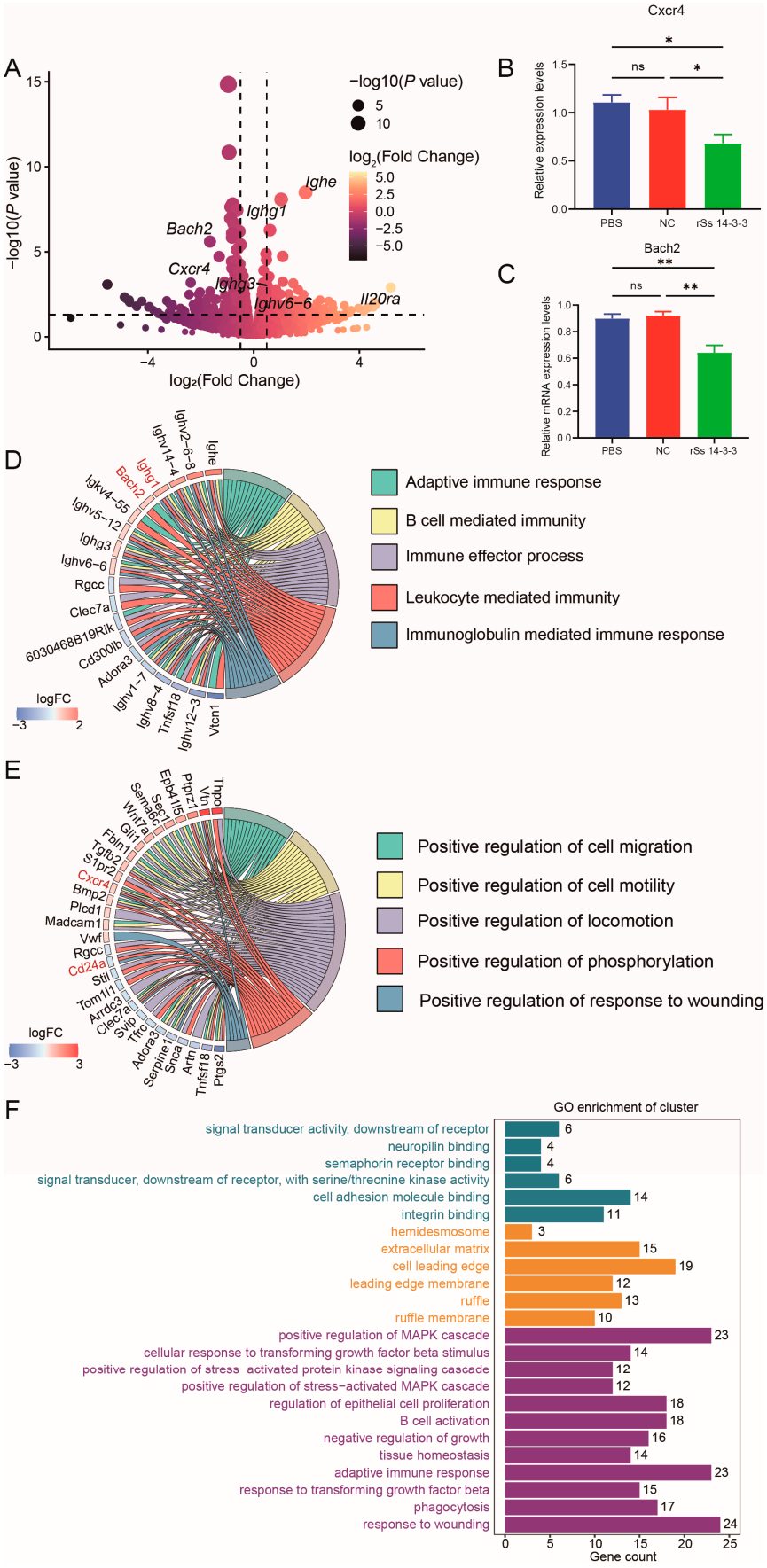


Figure 4. Transcriptomic analysis of mouse spleens following rSs14-3-3 immunization. (**A**) Volcano plot showing differentially expressed genes (DEGs) between rSs14-3-3 immunization group and

NC group. Dot color indicates the log2 (fold-change). Dot size indicates the log10 (p values). |log2 (fold-change)| > 0.5 and p value < 0.05 are identified as DEGs. (**B**,**C**) Relative mRNA expression levels of Cxcr4 and Bach2 were measured by RT-qPCR. (**D**,**E**) Chord plot shows terms related to immunobiological processes in GO enrichment analysis of DEGs. (**F**) The top GO terms enriched in DEGs. Colors distinguish the three Gene Ontology categories (BP, CC, MF).Asterisks indicate statistically significant differences: * $p < 0.05$, ** $p < 0.01$; ns, not significant.

4. Discussion

In the present study, we successfully expressed and purified recombinant Ss14-3-3 in a eukaryotic expression system and confirmed its identity by mass spectrometry. Its immunological characteristics were subsequently evaluated at three complementary levels: recognition by sera from naturally infected patients, antibody responses following mouse immunization, and immunization-associated splenic transcriptional alterations. The principal findings demonstrated that rSs14-3-3 was recognized by sera from patients with strongyloidiasis, induced specific IgG1 and IgG2a responses in mice when administered with Freund's adjuvant, and was associated with transcriptional changes involving adaptive immunity and B-cell-related pathways. Together, these findings demonstrate the immunogenicity of rSs14-3-3 in the presence of Freund's adjuvant and suggest that it warrants further evaluation as a candidate antigen.

The 14-3-3 protein family comprises highly conserved eukaryotic regulatory proteins with extensive protein-interaction capabilities and important functions in signaling, cell differentiation, and immune regulation [10]. Parasite-derived 14-3-3 proteins have been characterized in *Schistosoma japonicum*, *Clonorchis sinensis*, *Entamoeba histolytica*, and other parasites, where they participate in parasite development and host–parasite interactions [11–13]. Our findings further suggest that Ss14-3-3 may be associated with the regulation of immune-cell activation and migration, providing additional evidence supporting its potential value as a vaccine candidate. Structural prediction indicated that Ss14-3-3 predominantly consists of α-helices, consistent with the typical structural features of 14-3-3 family proteins. NetPhos analysis further predicted numerous potential serine, threonine, and tyrosine phosphorylation sites, suggesting that Ss14-3-3 may be subject to phosphorylation-dependent regulation.

In the present study, immunization with rSs14-3-3 was accompanied by alterations in transcriptional signals associated with immune-cell activation and migration. Previous studies have demonstrated that 14-3-3 proteins can influence T-cell differentiation and indirectly regulate cytokine production. In addition, they can modulate cytokine-related signaling through interactions with transcription factors, pattern-recognition receptors, and other receptors involved in inflammatory responses [14–16]. Parasite-derived 14-3-3 proteins have been detected on the parasite surface and in excretory/secretory products and are considered important components of host–parasite interactions. These proteins can induce the production of parasite-specific antibodies, including increased IgG responses [17]. Consistently, immunization with rSs14-3-3 in the present study resulted in pronounced increases in antigen-specific IgG subclasses. Serum antigen-specific antibody levels represent an important indicator of vaccine-induced immune responses. Such antibodies may interfere with parasite invasion of host cells and thereby contribute to reduced susceptibility to infection [18]. Our findings therefore demonstrate the strong immunogenicity of rSs14-3-3 and support further investigation of this protein as a potential vaccine antigen.

Previous studies have demonstrated that 14-3-3 proteins derived from several parasite species induce marked humoral and/or cellular immune responses and may confer partial protection in different experimental models. However, the patterns of immune polarization vary among parasite species. For example, 14-3-3 proteins from *Echinococcus granulosus* and *Trichinella spiralis* tend to induce relatively balanced IgG1/IgG2a responses,

whereas the *Toxoplasma gondii* 14-3-3 protein induces a predominantly Th1-type response characterized by IgG2a and IFN-γ production. Schistosome 14-3-3 proteins have also been shown to induce both humoral and cellular immune responses and confer moderate protection [17,19–21]. Notably, the increases in IgG1 and IgG2a were accompanied by changes in *Bach2* and *Cxcr4* expression. The opposite expression patterns of *Bach2* and *Cxcr4* may reflect biological variation between the separate sets of mice used for RNA-seq and RT-qPCR, together with differences in transcript quantification and normalization between the two assays. We therefore interpret the findings for these genes as assay-specific expression observations. BACH2 and CXCR4 have established roles in B-cell differentiation and migration, respectively [22,23]. These expression changes, together with the enrichment of B-cell-associated processes, suggest that the response to rSs14-3-3 immunization may involve B-cell-associated transcriptional changes. The prominent erythroid-associated genes *Alas2*, *Hbb-bt*, and *Hbb-bs*, together with enrichment of heme- and porphyrin-related processes, further indicate that the transcriptional response should not be attributed exclusively to B cells. Further studies are needed to determine their functional significance.

In addition, previous studies of *E. granulosus*, *T. gondii*, and *T. spiralis* have demonstrated the diagnostic potential of parasite-derived 14-3-3 proteins. In the present study, Ss14-3-3 was predominantly detected in the anterior region of *S. stercoralis*, was specifically recognized by sera from infected patients, and exhibited relatively distant phylogenetic relationships with human-derived 14-3-3 proteins. The IgG reactivity observed in clonorchiasis and schistosomiasis sera suggests potential cross-reactivity, consistent with the conservation of parasite 14-3-3 proteins. Our sequence comparisons identified similarities between portions of the predicted Ss14-3-3 B-cell epitopes and corresponding regions of 14-3-3 homologues from schistosomes and Clonorchis sinensis. These similarities provide a plausible basis for shared antibody recognition, although the cross-reactive epitopes have not been experimentally mapped. These additional clinical serum findings complement the mouse immunization results by characterizing antigen recognition and identifying a specificity limitation relevant to future antigen selection. Larger, clinically characterized cohorts, including patients with other helminth infections, are required to assess diagnostic performance and determine whether selection of less conserved epitopes could improve specificity.

Freund's adjuvant was used in the present study to establish an experimental model for evaluating immunogenicity. Previous studies of recombinant parasite proteins have demonstrated that vaccine efficacy can potentially be enhanced through antigen combinations or alternative formulations. Li et al. [17], for example, immunized mice with recombinant *E. granulosus* 14-3-3 formulated with Freund's adjuvant and observed marked changes in IgG1 and IgG2a levels. Yang et al. [24] immunized mice with recombinant *T. spiralis* 14-3-3 formulated with ISA50V2 adjuvant and observed not only antigen-specific IgG subclass responses but also elevated secretion of cytokines including IFN-γ, IL-2, and IL-4 by splenocytes. In the present study, only rSs14-3-3 formulated with Freund's adjuvant was evaluated. The present findings extend the characterization of Ss14-3-3 reported by Sánchez-Palencia et al. [9]. Following immunization with bacterially expressed rSs14-3-3 and experimental *S. venezuelensis* infection, that study observed increased splenic transcript levels of IL-10, TGF-β, IL-13, and TNF-α. Protection was not observed, and higher worm burdens and fecal egg counts suggested immunomodulation potentially favoring parasite establishment. Our study provides complementary evidence through human serum recognition of yeast-expressed rSs14-3-3, antigen-specific IgG1 and IgG2a responses following mouse immunization, and associated whole-spleen transcriptional changes involving B-cell-related and erythroid-associated processes. Reactivity with sera from patients with other helminth infections also identifies potential cross-reactivity relevant to diagnostic

applications. Differences in expression system, adjuvant formulation, mouse strain, and infection status limit direct comparisons between the studies.

Several limitations should be considered when interpreting our findings. The relatively small number of human serum samples limits the conclusions regarding the diagnostic potential of Ss14-3-3. Because the ELISA cutoff was derived from three healthy control sera, its diagnostic performance requires evaluation in a larger, independent cohort. In addition, the immunological evaluation mainly focused on antibody responses and splenic transcriptional changes, and further cellular and functional studies will be needed to clarify the underlying mechanisms. Finally, as the present study was designed primarily to evaluate immunogenicity, protective efficacy was not directly assessed by an infection-challenge experiment. Future studies using appropriate infection models and alternative adjuvant formulations will help further define the protective potential of rSs14-3-3 [25–27].

5. Conclusions

In summary, this study further characterized the molecular and immunological features of the *S. stercoralis* 14-3-3 protein, demonstrated its recognition by human sera and its ability to induce antigen-specific humoral responses in mice, and identified associated whole-spleen transcriptional changes, providing additional evidence of its antigenicity and immunogenicity and laying a foundation for subsequent mechanistic studies.

Supplementary Materials: The following supporting information can be downloaded at: https://www.mdpi.com/article/10.3390/pathogens15111211/s1, Figure S1: Identification of specific genes in *Strongyloides stercoralis*; Figure S2: Bioinformatics analysis of *Strongyloides stercoralis* (*Ss*) 14-3-3; Figure S3: Identification of the eukaryotic expression properties of the *Strongyloides stercoralis* (*Ss*) 14-3-3 recombinant protein; Figure S4: Sequencing results of the recombinant plasmid; Figure S5: Enrichment analysis for DEGs; Table S1: Amino acid composition; Table S2: Cellular epitopes of Ss14-3-3; Table S3: Protein Mass Spectrometry Analysis of Ss14-3-3 Recombinant Protein; Table S4: OD value of patient serum antibodies at 450 nm; Table S5: DEGs between rSs14-3-3 group and NC group; Table S6: 36 FDR-significant genes for GO term enrichment; Table S7 DEGs for GO term enrichment; Table S8: GSEA analysis for DEGs.

Author Contributions: Conceptualization and supervision, X.F. and D.L.; methodology and investigation, Q.W., Q.B., Y.S., X.C., J.L. and J.S.; resources, L.T. and S.H.; formal analysis and visualization, Q.W., Q.B. and Y.S.; writing—original draft preparation, Q.W., Q.B. and Y.S.; writing—review and editing, X.F. and D.L.; funding acquisition, D.L. All authors have read and agreed to the published version of the manuscript.

Funding: This research was funded by the National Natural Science Foundation of China (82160394) and the Guangxi Natural Science Foundation (2025GXNSFAA069174).

Institutional Review Board Statement: Collection and use of clinical samples were approved by the Ethics Committee of Guangxi Medical University (approval no. 20210049, approved on 27 February 2021). All animal experimental procedures were approved by the Animal Ethics Committee of Guangxi Medical University (approval no. 202403005, approved on 12 March 2024).

Informed Consent Statement: Informed consent was obtained from all subjects involved in the study.

Data Availability Statement: The Ss14-3-3 protein sequence was retrieved from NCBI GenBank under accession number QWX95795.1. The other data that support the findings of this study are available on request from the corresponding author.

Acknowledgments: Special thanks go to my classmates for sharing valuable insights and resources.

Conflicts of Interest: The authors declare no conflicts of interest.

Abbreviations

The following abbreviations are used in this manuscript:

ADAD	Adjuvant adaptation system
ANOVA	Analysis of variance
BP	Biological process
BSA	Bovine Serum Albumin
CC	Cellular component
DEGs	Differentially expressed genes
ELISA	Enzyme-Linked Immunosorbent Assay
FDR	False discovery rate
GO	Gene Ontology
GSEA	Gene set enrichment analysis
MF	Molecular function
NC	Negative control
PBS	Phosphate-Buffered Saline
pLDDT	Predicted local distance difference test
rSs14-3-3	Recombinant *Strongyloides stercoralis* 14-3-3 protein
SDS-PAGE	Sodium dodecyl sulfate–polyacrylamide gel electrophoresis
Ss14-3-3	*Strongyloides stercoralis* 14-3-3 protein

References

1. Buonfrate, D.; Bisanzio, D.; Giorli, G.; Odermatt, P.; Fürst, T.; Greenaway, C.; French, M.; Reithinger, R.; Gobbi, F.; Montresor, A.; et al. The Global Prevalence of *Strongyloides stercoralis* Infection. *Pathogens* **2020**, *9*, 468. [CrossRef] [PubMed]
2. Gandasegui, J.; Onwuchekwa, C.; Krolewiecki, A.J.; Doyle, S.R.; Pullan, R.L.; Enbiale, W.; Kepha, S.; Hatherell, H.A.; van Lieshout, L.; Cambra-Pellejà, M.; et al. Ivermectin and albendazole coadministration: Opportunities for strongyloidiasis control. *Lancet Infect. Dis.* **2022**, *22*, e341–e347. [CrossRef] [PubMed]
3. Raheel, H.; Kopalakrishnan, S.; Bhasker, S.; Makhani, L.; Clarke, S.; Nicholas, M.N.; Mufti, A.; Boggild, A.K. Inflammatory bowel disease later diagnosed as strongyloides colitis in migrants to Canada: A case series. *Ther. Adv. Infect. Dis.* **2023**, *10*, 20499361231162719. [CrossRef] [PubMed]
4. Esperante, D.; Flisser, A.; Mendlovic, F. The many faces of parasite calreticulin. *Front. Immunol.* **2023**, *14*, 1101390. [CrossRef] [PubMed]
5. Zhang, Z.; Song, X.; Deng, Y.; Li, Y.; Li, F.; Sheng, W.; Tian, X.; Yang, Z.; Mei, X.; Wang, S. Trichomonas vaginalis adhesion protein 65 (TvAP65) modulates parasite pathogenicity by interacting with host cell proteins. *Acta Trop.* **2023**, *246*, 106996. [CrossRef] [PubMed]
6. More, K.R.; Kaur, I.; Giai Gianetto, Q.; Invergo, B.M.; Chaze, T.; Jain, R.; Huon, C.; Gutenbrunner, P.; Weisser, H.; Matondo, M.; et al. Phosphorylation-Dependent Assembly of a 14-3-3 Mediated Signaling Complex during Red Blood Cell Invasion by *Plasmodium falciparum* Merozoites. *mBio* **2020**, *11*, e01287-20. [CrossRef] [PubMed]
7. Xiong, C.; He, W.; Xiao, J.; Hao, G.; Pu, J.; Chen, H.; Xu, L.; Zhu, Y.; Yang, G. Assessment of the Immunoprotective Efficacy of Recombinant 14-3-3 Protein and Dense Granule Protein 10 (GRA10) as Candidate Antigens for Rabbit Vaccines against Eimeria intestinalis. *Int. J. Mol. Sci.* **2023**, *24*, 14418. [CrossRef] [PubMed]
8. Masoori, L.; Falak, R.; Mokhtarian, K.; Bandehpour, M.; Razmjou, E.; Jalallou, N.; Jafarian, F.; Akhlaghi, L.; Meamar, A.R. Production of recombinant 14-3-3 protein and determination of its immunogenicity for application in serodiagnosis of strongyloidiasis. *Trans. R. Soc. Trop. Med. Hyg.* **2019**, *113*, 326–331. [CrossRef] [PubMed]
9. Sánchez-Palencia, L.F.; Trelis, M.; López-Abán, J.; Galiano, A.; Vicente, B.; Del Olmo, E.; Muro, A.; Bernal, D.; Marcilla, A. Evaluation of the Immunomodulatory Effect of the Recombinant 14-3-3 and Major Antigen Proteins of *Strongyloides stercoralis* against an Infection by S. venezuelensis. *Vaccines* **2022**, *10*, 1292. [CrossRef] [PubMed]
10. Stevers, L.M.; Sijbesma, E.; Botta, M.; MacKintosh, C.; Obsil, T.; Landrieu, I.; Cau, Y.; Wilson, A.J.; Karawajczyk, A.; Eickhoff, J.; et al. Modulators of 14-3-3 Protein-Protein Interactions. *J. Med. Chem.* **2018**, *61*, 3755–3778. [CrossRef] [PubMed]
11. Liu, J.; Giri, B.R.; Chen, Y.; Cheng, G. 14-3-3 protein and ubiquitin C acting as SjIAP interaction partners facilitate tegumental integrity in Schistosoma japonicum. *Int. J. Parasitol.* **2019**, *49*, 355–364. [CrossRef] [PubMed]
12. Wang, X.; Chen, W.; Li, X.; Zhou, C.; Deng, C.; Lv, X.; Fan, Y.; Men, J.; Liang, C.; Yu, X. Identification and molecular characterization of a novel signaling molecule 14-3-3 epsilon in Clonorchis sinensis excretory/secretory products. *Parasitol. Res.* **2012**, *110*, 1411–1420. [CrossRef] [PubMed]
13. Agarwal, S.; Anand, G.; Sharma, S.; Parimita Rath, P.; Gourinath, S.; Bhattacharya, A. EhP3, a homolog of 14-3-3 family of protein participates in actin reorganization and phagocytosis in Entamoeba histolytica. *PLoS Pathog.* **2019**, *15*, e1007789. [CrossRef] [PubMed]

14. Bai, B.; Wang, T.; Zhang, X.; Ba, X.; Zhang, N.; Zhao, Y.; Wang, X.; Yu, Y.; Wang, B. PTPN22 activates the PI3K pathway via 14-3-3τ in T cells. *FEBS J.* **2023**, *290*, 4562–4576. [CrossRef] [PubMed]
15. Fernández-Orth, J.; Ehling, P.; Ruck, T.; Pankratz, S.; Hofmann, M.S.; Landgraf, P.; Dieterich, D.C.; Smalla, K.H.; Kähne, T.; Seebohm, G.; et al. 14-3-3 Proteins regulate K(2P) 5.1 surface expression on T lymphocytes. *Traffic* **2017**, *18*, 29–43. [CrossRef] [PubMed]
16. Soini, L.; Leysen, S.; Davis, J.; Westwood, M.; Ottmann, C. The 14-3-3/SLP76 protein-protein interaction in T-cell receptor signalling: A structural and biophysical characterization. *FEBS Lett.* **2021**, *595*, 404–414. [CrossRef] [PubMed]
17. Li, Z.J.; Wang, Y.N.; Wang, Q.; Zhao, W. *Echinococcus granulosus* 14-3-3 protein: A potential vaccine candidate against challenge with *Echinococcus granulosus* in mice. *Biomed. Environ. Sci.* **2012**, *25*, 352–358. [CrossRef] [PubMed]
18. Li, S.; Zhang, N.; Liu, S.; Li, J.; Liu, L.; Wang, X.; Li, X.; Gong, P.; Zhang, X. Protective Immunity Against Neospora caninum Infection Induced by 14-3-3 Protein in Mice. *Front. Vet. Sci.* **2021**, *8*, 638173. [CrossRef] [PubMed]
19. Meng, M.; He, S.; Zhao, G.; Bai, Y.; Zhou, H.; Cong, H.; Lu, G.; Zhao, Q.; Zhu, X.Q. Evaluation of protective immune responses induced by DNA vaccines encoding Toxoplasma gondii surface antigen 1 (SAG1) and 14-3-3 protein in BALB/c mice. *Parasit. Vectors* **2012**, *5*, 273. [CrossRef] [PubMed]
20. Schechtman, D.; Tarrab-Hazdai, R.; Arnon, R. The 14-3-3 protein as a vaccine candidate against schistosomiasis. *Parasite Immunol.* **2001**, *23*, 213–217. [CrossRef] [PubMed]
21. Zhang, Y.; Taylor, M.G.; Johansen, M.V.; Bickle, Q.D. Vaccination of mice with a cocktail DNA vaccine induces a Th1-type immune response and partial protection against Schistosoma japonicum infection. *Vaccine* **2001**, *20*, 724–730. [CrossRef] [PubMed]
22. Shao, W.; Wang, Y.; Fang, Q.; Shi, W.; Qi, H. Epigenetic recording of stimulation history reveals BLIMP1-BACH2 balance in determining memory B cell fate upon recall challenge. *Nat. Immunol.* **2024**, *25*, 1432–1444. [CrossRef] [PubMed]
23. Giorgiutti, S.; Rottura, J.; Korganow, A.S.; Gies, V. CXCR4: From B-cell development to B cell-mediated diseases. *Life Sci. Alliance* **2024**, *7*, e202302465. [CrossRef] [PubMed]
24. Yang, J.; Zhu, W.; Huang, J.; Wang, X.; Sun, X.; Zhan, B.; Zhu, X. Partially protective immunity induced by the 14-3-3 protein from Trichinella spiralis. *Vet. Parasitol.* **2016**, *231*, 63–68. [CrossRef] [PubMed]
25. Herbert, D.R.; Nolan, T.J.; Schad, G.A.; Abraham, D. The role of B cells in immunity against larval *Strongyloides stercoralis* in mice. *Parasite Immunol.* **2002**, *24*, 95–101. [CrossRef] [PubMed]
26. Charuchaibovorn, S.; Sanprasert, V.; Nuchprayoon, S. The Experimental Infections of the Human Isolate of Strongyloides Stercoralis in a Rodent Model (The Mongolian Gerbil, Meriones Unguiculatus). *Pathogens* **2019**, *8*, 21. [CrossRef] [PubMed]
27. Viney, M.; Kikuchi, T. Strongyloides ratti and S. venezuelensis rodent models of Strongyloides infection. *Parasitology* **2017**, *144*, 285–294. [CrossRef] [PubMed]

Disclaimer/Publisher's Note: The statements, opinions and data contained in all publications are solely those of the individual author(s) and contributor(s) and not of MDPI and/or the editor(s). MDPI and/or the editor(s) disclaim responsibility for any injury to people or property resulting from any ideas, methods, instructions or products referred to in the content.